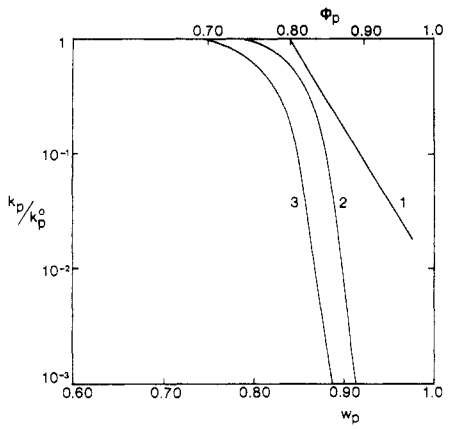

Figure 5. Variation of the propagation rate constant with the weight fraction of polymer: (1) experimental results; (2, 3) theoretical predictions of the free volume theory with $D_{MO} = 1 \times 10^{-5}$ and 1×10^{-6} cm^2 s^{-1}, respectively.

transition point eq 4 and 5 predict an extremely rapid decrease in k_p with w_p. The experimentally determined decrease in k_p is much less dramatic, resulting in the theoretical values for k_p being several orders of magnitude less than the observed values if $w_p > 0.90$. Clearly, eq 4 and 5 must be used with caution at high weight fractions of polymer.

Conclusions

It is apparent that quantitative ESR measurements in combination with dilatometric data provide a method with considerable potential for the measurement of propagation rate coefficients. The values obtained are essentially free of any model-based assumptions. Absolute accuracy is about ±40%, while relative accuracy (as the variation of k_p with w_p) is ±25%. For methyl methacrylate at 50 °C, we obtained

$$k_p = k_p^0, \quad 0.33 \le w_p \le 0.84$$
$$= k_p^0 \exp\{-29.8[w_p - 0.84]\}, \quad 0.84 > w_p \ge 0.99$$

where $k_p^0 = 790 \pm 300$ dm^3 mol^{-1} s^{-1}. These results show that for propagation a mechanistic transition occurs at the glass transition point ($w_p = 0.84$), so that the rate-determining step becomes the diffusion of monomer to the propagation site. It is particularly noteworthy that the technique described here can be applied to systems containing very high proportions of polymer; and indeed, the experimental uncertainties decrease with increasing w_p.

Acknowledgment. The generous support of the Australian Research Grant Scheme is gratefully acknowledged. We deeply appreciate useful correspondence with Professor Donald Sundberg.

References and Notes

(1) Ballard, M. J.; Gilbert, R. G.; Napper, D. H.; Pomery, P. J.; O'Donnell, J. H. *Macromolecules* **1984**, *17*, 504.
(2) Bengough, W. I.; Melville, H. W. *Proc. R. Soc. London, A*: **1955**, *230*, 429. Hayden, P.; Melville, H. W. *J. Polym. Sci.* **1960**, *43*, 201.
(3) Ballard, M. J.; Napper, D. H.; Gilbert, R. G. *J. Polym. Sci., Polym. Chem. Ed.* **1984**, *22*, 3225.
(4) Horie, K.; Mita, I.; Kambe, H. *J. Polym. Sci., Polym. Chem. Ed.* **1968**, *6*, 2663.
(5) Friis, N.; Hamielec, A. E. *ACS Symp. Ser.* **1976**, *24*, 82.
(6) Earnshaw, R.; O'Donnell, J. H.; Whittaker, A. K., to be published.
(7) Gardon, J. L. *J. Polym. Sci., Polym. Chem. Ed.* **1968**, *6*, 2851.
(8) Soh, S. K.; Sundberg, D. C. *J. Polym. Sci., Polym. Chem. Ed.* **1982**, *20*, 1299, 1315.
(9) Korus, R.; O'Driscoll, K. F. In *Polymer Handbook*, 2nd ed.; Brandrup, J., Immergut, E. H., Eds.; Wiley-Interscience: New York, 1975.
(10) Kamachi, M.; Kohno, M.; Kuwae, Y.; Nozakura, S. *Polym. J. (Tokyo)* **1982**, *14*, 749.
(11) Soh, S. K.; Sundberg, D. C. *J. Polym. Sci., Polym. Chem. Ed.* **1982**, *20*, 1331.
(12) Rabinowitch, E. *Trans. Faraday Soc.* **1937**, *33*, 1225.
(13) Sundberg, D. C., 1985, personal communication.

Changes of Liquid Crystalline Polymer Structure with Temperature. 6. Distortion of One-Dimensional Order in Smectic B Polymer

Vladimir Tsukruk, Valery Shilov, and Yury Lipatov*

Institute of Macromolecular Chemistry, Academy of Sciences, UkrSSR, Kiev 252160, USSR.
Received March 27, 1984

ABSTRACT: The character of one-dimensional order in a smectic polymer with mesogenic side groups and long spacers was studied by means of SAXS experiments, polarized microscopy, and electron microscopy over a wide temperature range, including the clearing temperature. It was demonstrated that the electron density distribution along the normal-to-smectic plane is a complicated function, characteristic of three-component systems. Such state is due to microphase separation of different fragments of macromolecules. The damping of correlation in smectic layer arrangements has an exponential form with correlation lengths of 460–600 Å. The temperature increase leads to decreasing layer-packing perfection and thermal expansion of interlayer and intralayer packing. In the isotropic state a weak fluctuation of electron density, which was associated with the correlation hole effect, was observed.

Introduction

It is quite evident that the changes of one-dimensional order in layered liquid crystalline (LC) polymers (i.e., smectics) with temperature, especially in the vicinity of phase transitions, have not been sufficiently investigated up to the present time. The available data indicate a decrease of the orientational order parameter during transition into the isotropic melt state (near the clearing points T_{cl}).[1-3] For some smectic polymers, as has been found in ref 4–7, the degree of perfection of the layered order increases with temperature rise. However, up to now the nature of the temperature dependence of structural

0024-9297/86/2219-1308$01.50/0

parameters on translational order, that is, the amplitude of the one-dimensional density wave along the normal-to-layer plane and the correlation length characterizing the extent of layered-order regions, ξ, for smectic polymers is unknown. The first of these characteristics is the absolute value of the translational order parameter ψ in the de Gennes–McMilian theory.[8] The second characteristic determines the rate of correlation damping in smectic layer arrangements with increasing distance between them.[8-10]

In low molecular weight smectics the correlation in layer arrangement decreases by a power law: $G(x) \sim x^{-n}$ (where $G(x)$ is the so-called correlation function and x is the distance between smectic layers). The power law of correlation damping in one-dimensional systems with thermal fluctuations of order was substantiated by Landau.[11,12] At the same time correlation in the arrangement of structural elements in low-ordered, liquidlike systems, as shown by Debye,[13] decreases considerably faster, according to the exponentional law $G(x) \sim \exp(-x/\xi)$. The same type of correlation damping was established by Vonk[14] for layered structures with a high content of paracrystalline defects.

In this paper we aim at solving the problem of determining the nature of changes of the above-indicated parameters of translational order (one-dimensional wave amplitudes and correlation lengths) in the smectic B polymer with perfect intralayer packing of mesogenic groups during the transition from glassy state into LC state and in the region of T_{cl} and below and above this point.

Experimental Procedures

A smectic B polymer with phenyl benzoate side groups and a flexible aliphatic spacer of ten methylene links was investigated:

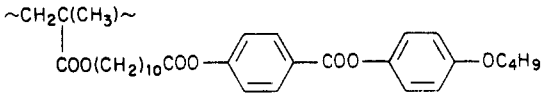

The synthesis of the polymer has been described earlier.[15] The molecular weight of the polymer is $M_n = 1.14 \times 10^5$; the clearing temperature is $T_{cl} = 129$ °C.[16] Type of mesomorphic order was established by wide-angle X-ray scattering.[5]

The samples for investigation were prepared from benzene solution in the form of fine films on Mylar (registered trademark of Du Pont) substrate by multiple wetting and removal of the solvent. Sample thickness was 0.5 mm. To remove the residual solvent and to anneal the polymer, it was stored under vacuum at 125 °C for 4–5 h and then slowly (8–10 h) cooled to room temperature.

Polarized microscopic studies were carried out by means of microscope MIN-8 with a heating stage. Electron-microscopic data were obtained on JEM-100C microscope. Samples for electron-microscopic studies were prepared by replica method (for details see ref 3 and 4).

The small-angle X-ray scattering (SAXS) curves of the polymer investigated were obtained with a Rigaku-Denki type diffractometer (called DRAM-2.0) by automatic step-by-step scanning.[17a-c] X-ray photopatterns of the oriented samples were obtained on a flat plate in a vacuum chamber.

During recording of SAXS curves no Soller slits were used. As is known, in diffractometers with slit collimation systems the Soller slits are used sometimes to decrease the smearing of SAXS curves.[17a-d] But the use of Soller slits leads to a sharp decrease of scattering intensity, especially on the tail of the SAXS curve. In this case an increase of statistical errors (at the same experimental time) leads to great uncertainity in the estimation of transition-zone thickness.[17d] At the same time, a greater scattering intensity in the diffractometer without Soller slits allows determination of the scattering curve with great accuracy (with statistical deviations from 0.1 to 2% on the curve tail). Further, accurate smoothing and desmearing of experimental data with high statistical reliability allow one to obtain a reliable point collimation curve.[17a,b,e] According to Kratky,[17b] the use of Soller slits is quite efficient only with a high-powder rotating anode X-ray source. Otherwise, the use of Soller slits does not compensate for the great difficulties in obtaining statistically satisfactory data, especially during estimation of transition-zone thickness from the SAXS curve tail.[17d,e] Taking into account these circumstances, we used in our experiments a conventional slit system[17a,b] without Soller slits.

SAXS curves for the sample were obtained within the range of angles from 0.04° to 6°; the slit width and the scanning step size were varied within the limits 100–800 μm and 0.02°–0.05°, respectively. Scannings were repeated 5–7 times, and the total number of counts in every scattering angle were 2×10^3 to 3×10^4. Copper radiation filtered by nickel foil was employed in the diffractometer and in the photochamber. To detect scattering radiation in the diffractometer a scintillation detector and impulse-height analyzer were used. Tube operating conditions were 30 kV and 50 mA.

For estimation of the accuracy of the experimental scattering curve a relation $\Delta S \leq {}^1/_2 D$ may be used,[17b] where ΔS is the maximum scanning step and D is the maximum obtainable dimensions of ordered microregions. In contrast, the calculation of transition-zone thickness with an accuracy of 10–20% requires statistical deviation on the curve tail of 1–2%.[17d] From these conditions we selected the above-mentioned experimental conditions: increments of 0.02° and number of counts on scattering tail greater than $(2\text{–}5) \times 10^3$.

Before the intensity curves were processed, the background scattering was subtracted, which, as a rule, did not exceed 10% of the total scattering intensity. For reduction to absolute units, a standard Kratky sample was used.[17a,b,18] The collimation correction was introduced by means of a deconvolution procedure taking into account the shape of the primary beam intensity distribution along the height.[17-19] The last were determined from photometric scanning of photopatterns of the primary beam and the convolution with height of receiving slit. The information zone near 2°, estimated from the instrumental function in accordance with ref 17a and b, is calculated to be 700 Å.

During studies the sample was placed between two Mylar films 10 nm thick and fitted in a microthermostat setup in the center of the vacuum chamber. The accuracy of temperature upkeep was 0.5 °C.

One-dimensional correlation functions $G_1(x)$ were obtained by Fourier-cosine transformation of intensity curves $I(s)$ multiplied by the Lorentz factor for lamellar structures s^2 [20-22]

$$G_1(x) = \int s^2 I(s) \cos(sx)\, ds \qquad (1)$$

$$s = 2 \sin \theta/\lambda$$

where 2θ is the diffraction angle and λ is the radiation wavelength.

For accurate determination of correlation function shape at the origin one must carry out a delicate separation of wide-angle scattering (including diffuse scattering from density thermal fluctuation) on the curve tail.[22,23] For this purpose we used a corresponding subroutine from the Vonk program.[23] We approximated a shape of wide-angle scattering I_{wa} by means of a power series in the form

$$I_{wa}(s) = a + \sum_n b_n S^n \qquad (2)$$

where $n = 2$, 4, or 6. After such approximation we subtracted I_{wa} from the experimental curve in all scanning interval.

The mean square of electron density fluctuation $\Delta\langle\rho^2\rangle$ was calculated from SAXS curves normalized to absolute units and reduced to point collimation:[17,18]

$$\Delta\langle\rho^2\rangle = 4\pi \int s^2 I(s)\, ds \qquad (3)$$

The experimental data were processed by computer ES-1020 on the Vonk program FFSAXS.[23]

Experimental Results

Under crossed polaroids at temperatures below T_{cl} batonnet-like structures are visible, which are characteristic of low molecular weight smectic LC (Figure 1 (top))[24] (in the figure, the structures are spread due to permanent displacement). In this figure an electron-microscopic

Table I
Structural Data for Polymer Studied

temp, °C	$\Delta\rho^2$, e²/Å⁶, 10^{-3}	d_1,[a] Å	d_2,[b] Å	S, Å			ξ	E, Å	α[c]	α'[d]
				l_1	l_2	l_3				
20	1.7	31.8	32.0	9	8.5	7	460	3	0.74	0.9
70	1.1	31.6	32.0	9	9	7	600	2	0.41	0.48
128	0.6	35.2	35.0	8	9	8	320	4	0.28	0.29
140	0.4	21	20(25)	9			15		0.18	

[a] d_1, calculated from scattering curves. [b] d_2, calculated from one-dimensional correlation curves (for 140 °C the d value obtained from three-dimensional correlation curve shown in parentheses). [c] α, degree of component segregation without taking into account the transition layers. [d] α' degree of component segregation taking into account the transition layers.

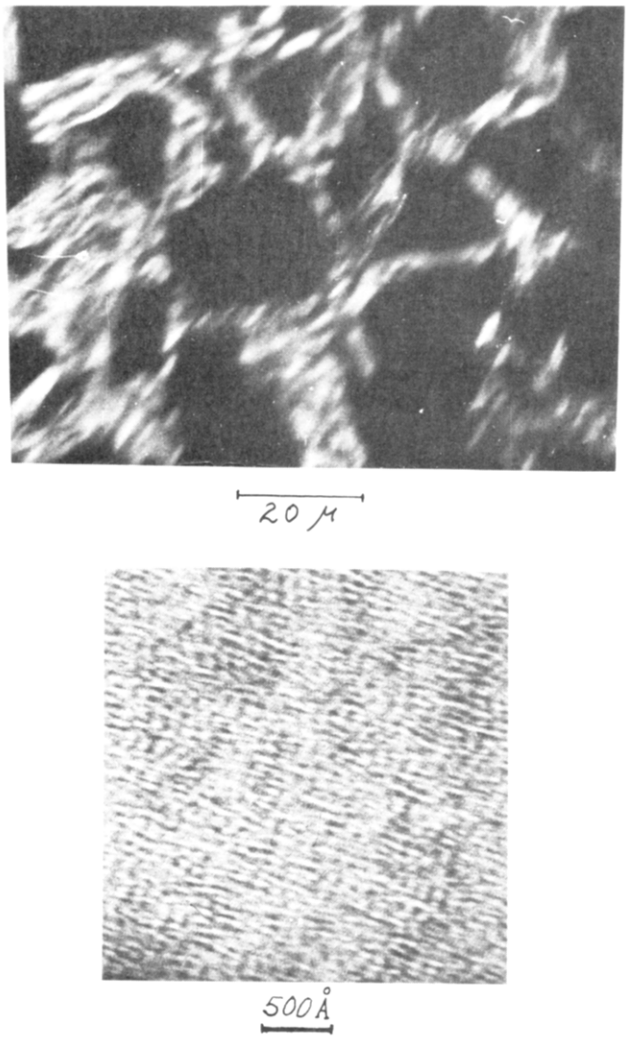

Figure 1. (Top) Polarized microscopic photograph of polymer in crossed polaroids at 126 °C (batonnets are spread on the picture due to their permanent displacements). (Bottom) Electron-microscopic photograph of layered structure in polymer studied.

photograph is presented, too (Figure 1 (bottom)). One can see a layered structure of smectic polymer of conventional type.[25]

Figure 2 shows SAXS curves for the polymer investigated in the glassy state (at room temperature), in LC state at 70 °C, in LC state near the transition to isotropic melt (at 128 °C), and in the state of isotropic melt at 140 °C. The SAXS curve of the glassy LC polymer exhibits an intensive sharp maximum at 2.6° and a considerably weaker diffuse maximum in the region of 5.2°.

The first maximum corresponds to the reflection from layered smectic planes with average periodicity of electron density distribution 32.0 ± 0.2 Å. The second maximum in the intensity curve, as can be seen from its position ($\theta_2/\theta_1 = 2.0$) as well as from its location in the X-ray tex-

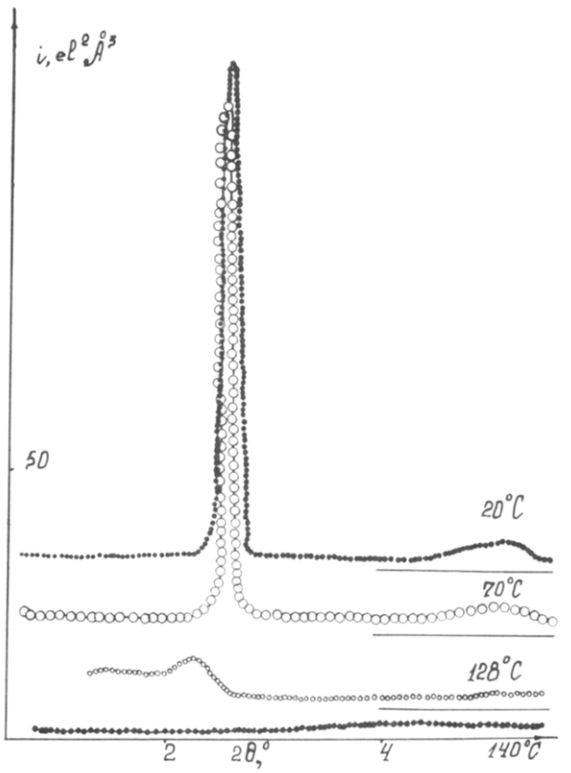

Figure 2. SAXS curves of polymer at various temperatures reduced to absolute units and desmeared.

ture patterns (both maxima are located in the equatorial plane)(Figure 3), is a next order of reflection from a unique system of planes.

As a result of polymer transition into LC state, the SAXS maxima become sharper, while their intensities change very little. Approaching the clearing point, the sharp first SAXS maximum turns into a weak diffuse maximum in the region of 2.5°. The transition to the isotropic state is accompanied by complete disappearance of this maximum and by the appearance on the intensity curve of a diffuse halo with the position of its peak corresponding to average periodicity of the order of 20 Å (Table I). This halo is also preserved after 10 h of treatment at 140 °C.

Characteristic changes are observed also in the correlation curves for this polymer at various temperatures (Figure 4). In the glassy state periodic oscillations gradually decreasing to zero at 680 Å are observed on the one-dimensional correlation curve $G_1(x)$. The periodicity of oscillations corresponds to a smectic plane spacing in 32 Å (Table I). With the rise of temperature to 70 °C the intensity of maxima on the correlation curve decreases, but the correlation damping occurs at a lesser rate than in the glassy state. As a result of this, $G_1(x)$ does not reach 0 even in the vicinity of the diffractometer information zone boundary. Close to T_{cl} the $G_1(x)$ correlation curve un-

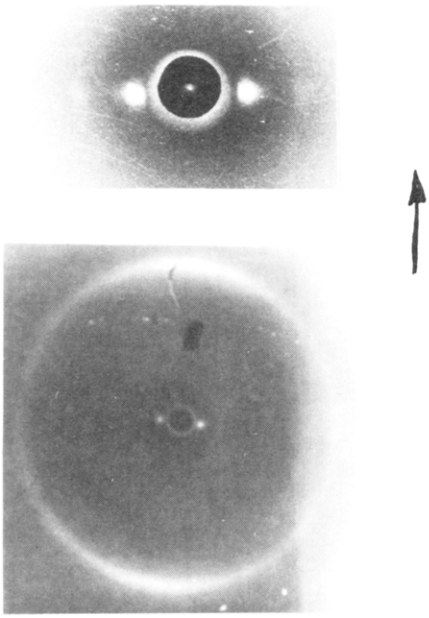

Figure 3. X-ray texture photographs of oriented polymer at wide (top) and small (bottom) angles (the orientation axis is vertical).

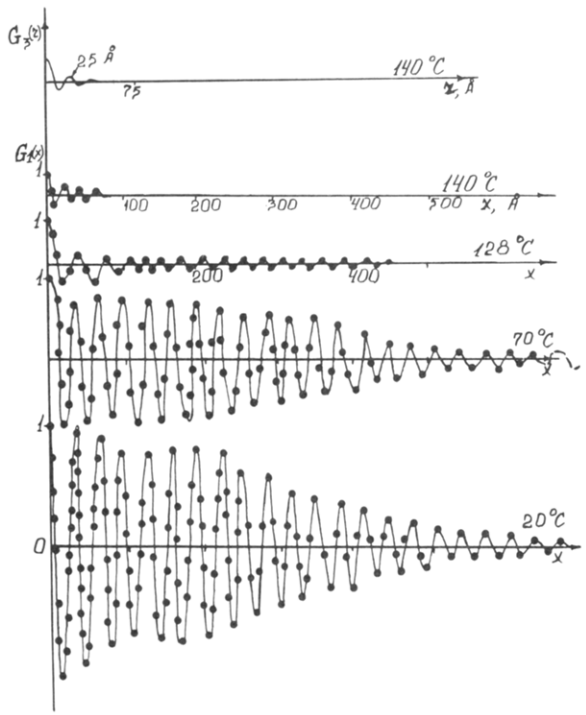

Figure 4. One-dimensional correlation curves $G_1(x)$ for a polymer at various temperatures (for 140 °C a three-dimensional correlation curve $G_3(r)$ is also shown).

dergoes considerable changes: the intensity of maxima drops a considerable degree, the oscillation periodicity increases to 35 Å, while the damping of $G_1(x)$ to 0 takes place at 400 Å. During transition to isotropic melt only two weak maxima with periodicity in 20 Å are observed in the one-dimensional correlation curve, and $G_1(x)$ attains 0 at 50 Å (Figure 4). Three-dimensional correlation curve $G_3(r)$ for polymer at 140 °C corresponding to structure with spherical symmetry was calculated, too (Figure 4).[23] This curve shows a weak peak at 25 Å, and $G_3(r)$ attains 0 at 40–45 Å.

An essential feature of the $G_1(x)$ curves, as compared to those obtained by us earlier for polymeric smectic of A and C types (with liquidlike intralayer order),[25-28] is the fact that in this case, in addition to the main density wave

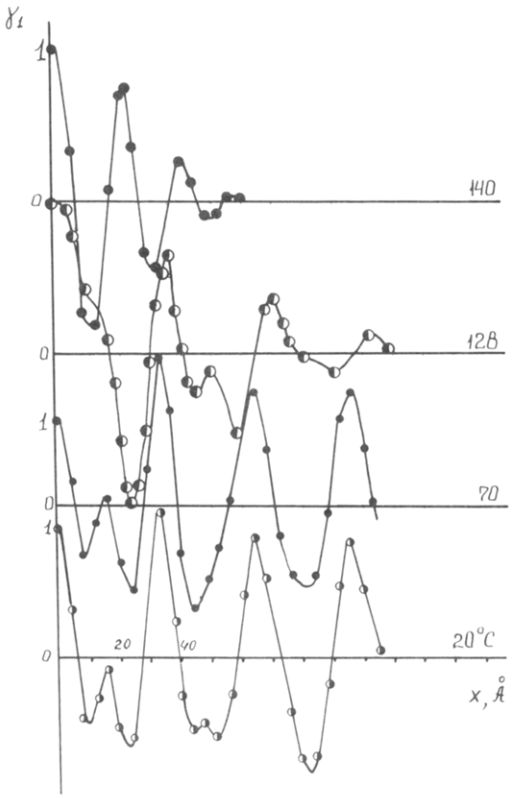

Figure 5. Normalized correlation functions $\gamma_1(x)$ in the region of small x.

of 32-Å periodicity, an additional peak appears on the zero maximum slope at 16 Å, which detects a complex form of electron density distribution into smectic layers.

This is illustrated well on the normalized correlation curves $\gamma_1(x) = G_1(x)/\Delta\langle\rho^2\rangle$ presented in Figure 5. This maximum is revealed quite distinctly within the limits of glassy and LC states. However, it degenerates in the vicinity of the clearing point into an arm on the slope of the zero maximum $\gamma_1(x)$ in the region of 15 Å. In the isotropic state all traces of this maximum disappear completely.

To estimate the reversibility of thermal changes in the LC polymer structure, we obtained SAXS curves after every 20 °C in heating the polymer to a temperature above T_{cl} and during polymer cooling to room temperature (Figure 6). As can be seen from this figure, the thermal changes of the scattering curve consisting of a shift toward the smaller angles and the disappearance of the SAXS maximum upon heating above T_{cl} is reversible, and the initial scattering curve is fully recovered when the polymer is cooled down to room temperature.

Discussion

Electron Density Distribution in Layered Structures. As is shown by calculation using the standard bond lengths and valence angles, the length of a fully stretched side group of the polymer investigated practically coincides with the thickness of smectic layer d, determined from the position of SAXS peak. This suggests for this polymer a one-layered pack of a usual type, as proposed earlier.[29-31] But the detailed consideration of electron density distribution along the normal-to-smectic plane leads to essentially another conclusion (see below). In real two-layered structures of this polymer the thickness of smectic layers is determined by the distance between the end groups of mesogenic side chains and it is 64 Å. The mesogenic groups are arranged normally to the smectic plane. The main chain over short distances is in trans zigzag confor-

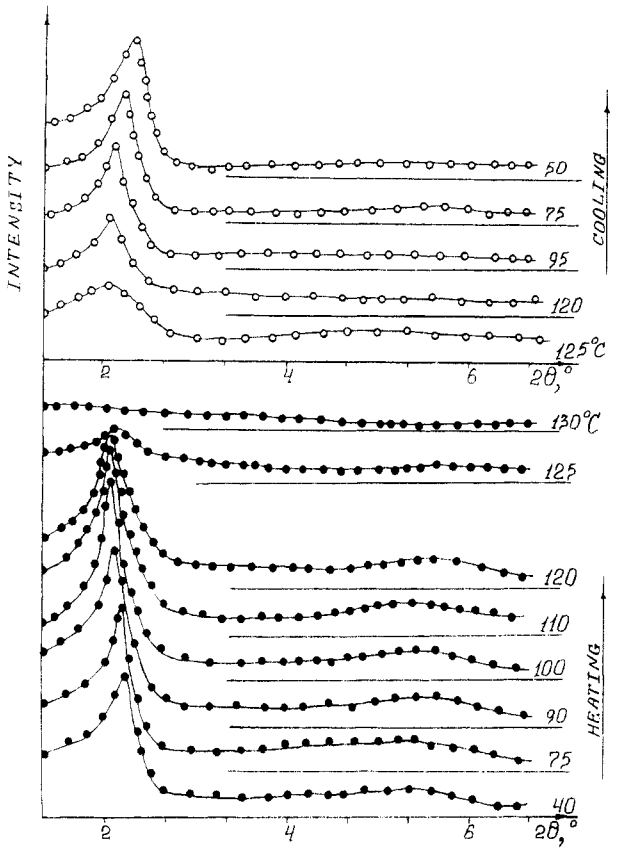

Figure 6. Variation of SAXS curves of a polymer during heating (full circles) and cooling (open circles).

mation.[29] Such type of layered pack is typical for a wide range of comblike polymers.[29] On corresponding X-ray texture photographs both SAXS reflections are situated at the equator while the wide-angle X-ray scattering is concentrated at the meridian (Figure 3). Such distribution of X-ray scattering shows that the mesogenic groups are really arranged normally to the smectic plane. In fact, the equator character of SAXS reflections shows that the smectic planes are directed along the texture axis. At the same time, the wide-angle scattering, corresponding to intralayer packing of mesogenic groups, is concentrated at the azimuthal angle $\varphi = 90°$ to the equator plane (on the meridian). Thus, the angle between the direction of mesogenic groups and the smectic plane is equal to 90° as well.

To define the density distribution function within the smectic layers along the normal-to-layer plane $\rho(x)$, it is necessary to analyze the profile of the zeroth and the additional maxima on the one-dimensional correlation functions $\gamma_1(x)$. For this purpose, in our previous works we used the Strobl–Schneider technique,[32] according to which $\rho(x)$ for polymers with lamellar structure is a periodic step function.[26-28,32] Areas with higher electron density correspond to regions containing the rigid nuclei of the mesogenic groups, whereas the areas with lower electron density correspond to regions where flexible fragments are situated. The periodicity in the arrangement of these regions coincides with the oscillation period on $\gamma_1(x)$. The length of the more dense region l_1 is determined in this method by the intersection point of the zeroth maximum $\gamma_1(x)$ with the axis x_0 by means of the relation

$$x_0 = d\varphi_1(1 - \varphi_1) \tag{4}$$

where $\varphi_1 = l_1/d$ is the fraction of regions with higher electron density and $\varphi_1 = 1 - \varphi_2$. This expression is true at $\varphi_1 \neq 0.5$.[32]

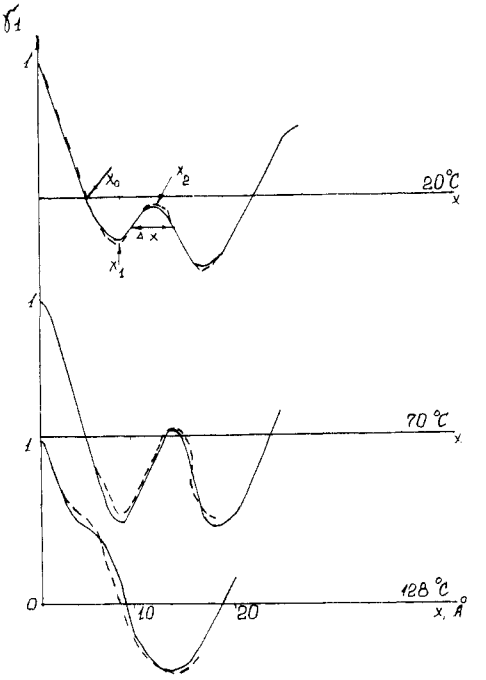

Figure 7. Modeling of zeroth maximum profile for $\gamma_1(x)$: solid line, experimental curves; dashed line, calculated curves.

The applications of this technique to the analysis of one-dimensional correlation functions made it possible to establish the nature of electron density distribution for a number of smectic polymers of the A and C types.[26-28] The complex shape of the $\gamma_1(x)$ profile for the investigated polymer with a long flexible spacer signifies, first of all, the nontrivial nature of the electron density profile in the layers. It is quite evident that determination of $\rho(x)$ by means of the usual Strobl–Schneider technique seems impossible.

Taking this fact into consideration, we modeled the shape of the zeroth maximum of $\gamma_1(x)$ for various $\rho(x)$. Here we used the method of finding the self-convolution of the function $\rho(x)$ described in detail by Hosemann.[33] The procedure as applied to smectic polymers will be described in detail elsewhere.[34]

A general outline of the procedure $\gamma_1(x)$ is as follows:

(1) Choose the initial density distribution proceeding from the chemical structure of the monomer repeat unit. Here, the regions of higher electron density were chosen from the results of the preceding investigations for the regions containing rigid nuclei of mesogenic groups and the main polymer chains.[27] Initially, the length chosen was assumed to be equal to the length of the corresponding fragments calculated by the standard bond lengths.

(2) Calculate zeroth maximum profile of $\gamma_1(x)$ by graphic selfconvolution of the chosen density distribution $\rho(x)$.[32]

(3) Compare the calculated and experimental profile $\gamma_1(x)$.

(4) Introduce the corresponding corrections to the distribution $\rho(x)$ and repeat the procedure until complete agreement between the modeled and experimental profiles of $\gamma_1(x)$ is obtained.

As shown by these calculations, the characteristic points on curve $\gamma_1(x)$ for determing the profile $\rho(x)$ are (1) the intercept on the right-hand side of $\gamma_1(x)$ with the axis of abscissa x_0, (2) the position of the complementary maximum x_2, (3) the position of the minimum x_1 between the slope of the zeroth and complementary maximum, and (4) the complementary maximum width x (Figure 7). The basic variable parameters of $\rho(x)$ in the adjustment process are the length and position of regions with higher electron

density and the ratio of densities in various regions. The model also takes into account the nonzero thickness of the transition zone (E) between regions of differing electron densities.[34-37] Within the limits of the linear-gradient Vonk model[34] this value is determined independently from curvature analysis of the zeroth maximum profile in the vicinity of $x = 0$:

$$E = 2\frac{\partial\gamma_1(x)}{\partial x}\left(\frac{\partial^2\gamma_1(x)}{\partial x^2}\right)^{-1}_{x\to 0} \quad (5)$$

The value of E is the width of the transition zone as shown on Figure 8 for sigmoidal distribution of density in this region.

Figure 7 shows experimental and calculated profiles $\gamma_1(x)$ obtained at the best agreement, and Figure 8 illustrates the most successful profiles of electron density distribution for this polymer at various temperatures. The model curves of electron density distribution $\rho(x)$ exhibit a characteristic feature distinguishing them from the $\rho(x)$ determined earlier for polymers with directly coupled mesogenic groups.[26-28] This feature consists of the presence of two regions with higher electron density, ρ_1, and ρ_3. One of these regions is connected with the packing of rigid nuclei of the mesogenic groups and is 9 Å long; the second region is 8 Å long and is determined by the packing of main methacrylate chains and the adjacent sections of the flexible spacers. The packing density of the rigid nuclei of mesogenic groups ρ_1 is higher than the packing density of main chains ρ_3. The one difference of "packing density" from trivial "density" is the unit of measure: during calculation instead of g/cm^3 the e/Å^3 unit is used. In the region of butyl endgroups packing a drop of electron density is observed (Figure 8). Butyl end groups are almost completely arranged in the transition zone between the rigid nuclei region and the packing minima between neighboring layers (Figure 8).

Extinction Law for SAXS Curve. The typical form of electron density distribution in the region of smectic layer $\gamma_1(x)$ for a given polymer makes it possible to suppose the existence of two-layer packing of mesogenic groups with periodicity of 64 Å. This fact contradicts the conclusion about realization of usual one-layer packing, which may be done on the basis of small-angle scattering pictures only.[29,30] In fact, in the case of two-layer packing there should be seen a small-angle diffraction maxima with a period of 64 Å. However, this is not true.

Let us consider this discrepancy in more detail. It is known that the scattering function $F(s)$ may be presented as follows 17a

$$F(s) \sim |f(s)|^2\widetilde{Z(s)|S(s)|^2} \quad (6)$$

where $f(s)$ is the structural factor of separate scattering elements (in our case, separate smectic layer), determined by Fourier transform of electron density distribution in the layer $\rho(x)$, $Z(s)$ is the interference function, and $|S(s)|^2$ is the form factor of microregions of coherent scattering (layered packs). For large dimensions of these microregions (our case) the contribution of variation in $|S(s)|^2$ into $F(s)$ is nonessential and eq 6 transforms in[17a]

$$F(s) \sim |f(s)|^2 Z(s) \quad (7)$$

For the system formed by plane smectic layers the interference function $Z(s)$ is a Laue function different from 0 at large N only in the region $S_n = \pm n/d$. This function presents itself a set of sharp peaks, their heights being proportional to N at $S_1 = 1/d$, $S_2 = 2/d$. ... The scattering function is determined by the value of the structure factor

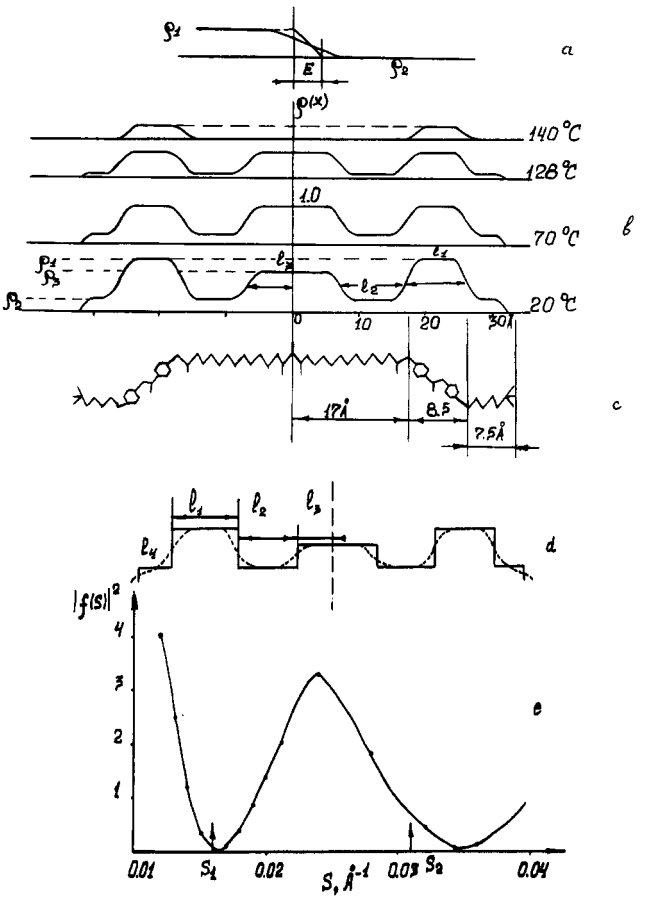

Figure 8. Density distribution (as used) in transition zone and measure of transition-zone width E, (a); electron density distribution along the normal-to-layer plane $\rho(x)$ at various temperatures (b); corresponding model of layered packing of mesogenic side groups (c); scheme of electron density distribution for calculation of structural factor $f(s)$ (d); angle dependence of structural factor for two-layered packing (e).

in those points of scattering vector s where $Z(s)$ has values of $S = \pm n/d$ different from 0. In such a way the form $f^2(s)$ determined the amplitude of reflections of various orders in points $s = \pm n/d$. Let us calculate the form of structure factor $f(s)$ for a given distribution of electron density in the layer $\rho(x)$ (Figure 8d). To simplify calculations we shall take instead of complicated profile $\rho(x)$ the set of corresponding rectangles of height ρ_1, ρ_2, and ρ_3 and dimension l_1, l_2, l_3, and l_4 (Figure 8d). It is shown in ref 17a that a change (really not taking into account the transition zones) does not influence profiles of the main reflections but changes the "tail" of small-angle scattering. For the model presented in Figure 8d the structure factor may be described in the form[17b]

$$f(s) = \int_{-d}^{d}\rho(x)\exp(2\pi isx)\,dx \quad (8)$$

or after corresponding transformations

$$f(s) = (1/\pi s)[(\rho_3 - \rho_2)\sin(2\pi s l_3) - (\rho_1 - \rho_2)\sin(2\pi s(l_2 + l_3)) + (\rho_1 - \rho_2)\sin(2\pi s(l_1 + l_2 + l_3)) + \rho_2\sin(2\pi s(l_1 + l_2 + l_3 + l_4))] \quad (9)$$

The angle dependence of the structure factor has been calculated from (9) by using for ρ_1, ρ_2, and ρ_3 the values discussed below. Values for l_1, l_2, l_3, and l_4 were taken from Table I. As is seen from the dependence of $f^2(s)$ (Figure 8c), the structure factor becomes equal to 0 at points $s = 0.015$ Å^{-1} and has a small value near 0.05 Å^{-1}, i.e., those points of scattering vector where the interference function $Z(s)$ for two-layer packing should give the first and third

orders of reflection. At the same time $f^2(s)$ is distinct from 0 at $s = 0.031$ Å^{-1}, corresponding to the second order of reflection from two-layer structure. Thus, first and third orders of reflection should be absent in the full scattering function, only second order of reflection being left from the plane system with period 64 Å. This fact is the result of the nontrivial form $\rho(x)$, which leads to extinction of first and third orders of reflection from two-layer packing. The extinction of reflections of different orders was described earlier for smectic structures.[29] Thus, thorough analysis of X-ray scattering data allows the conclusion to be drawn that in the polymer under investigation the two-layer packing of macromolecules is realized, but not one-layered packing as it was supposed earlier.[29-31]

Microphase Separation in Smectic Polymer. The mean square of the electron density fluctuation $\Delta\langle\rho^2\rangle$, which is directly related to the difference of packing densities in various regions of the layered structure, is determined from SAXS data.[17a] At the same time $\psi = (\Delta\langle\rho^2\rangle)^{1/2}$ is (in the approach used in ref 8) the amplitude of a one-dimensional density wave along the normal-to-smectic layer plane. In itself the value in absolute units carries little information. Apparently it is necessary to change over to a relative scale. Such changeover is easily done, and the corresponding parameter, referred to as a degree of segregation α,[38-40] is widely used to characterize block-polymer systems.

In the case of smectic LC polymers, the applicability of the parameter α is determined by the fact that these polymers may be considered to be specific block-polymer systems (multi-miniblock polymers) in which the layer order is established due to microphase separation of flexible and rigid macromolecular fragments.[26] In changing over to the relative scale, $\Delta\rho_0^2$ calculated for an ideal system is used as a reference point. The latter implies a system with sharp interfaces between regions of various electron density, ρ_i, equal to densities of pure components.[17a,34-37] In the case of three regions differing in their densities ρ_1, ρ_2, and ρ_3 with volume fractions l_1, l_2, and l_3, respectively, the following expression for $\Delta\langle\rho_0^2\rangle$ is true:[17]

$$\Delta\langle\rho_0^2\rangle = \varphi_1\varphi_2\Delta\langle\rho_{12}^2\rangle + \varphi_2\varphi_3\Delta\langle\rho_{23}^2\rangle + \varphi_1\varphi_2\Delta\langle\rho_{13}^2\rangle \quad (10)$$

To estimate $\Delta\langle\rho_0^2\rangle$ it is necessary either to measure the densities of the model compounds corresponding to given components or to evaluate them by calculation, as described in detail in ref 4. The latter procedure requires knowledge of paracrystalline parameters and the packing symmetry of mesogenic groups, obtainable from ref 5. For the given polymer we calculated the values proceeding from the parameters offered in ref 5, and for ρ_3 (the main chain density packing) the packing density of "pure" methacrylate macromolecules (PMMA) was used. The last assumption is supported by the known results for comblike polymers with long flexible side groups, which show that the structure of the main methacrylate chains is independent from the packing of side chains.[29]

The value $\alpha = \Delta\langle\rho_2\rangle/\Delta\langle\rho_0^2\rangle$ is the very measure of structure deviation in the given system from the ideal. The calculations show that α may vary from values close to 0 in fully disordered systems to values close to 1 in systems with perfect order (with complete microphase separation). Here, the value $\psi = \alpha^{1/2}$ is the measure of remoteness from the maximally possible wave amplitude of one-dimensional density. Value α, as is known from ref 17a, decreases due to both the presence in the system of layered-packing defects and the transition zones of nonzero thickness. The latter effect may be easily accounted for when the transition-layer fraction φ_E is known ($\varphi_E = 2E/d$).[40] In the case of lamellar structure instead of relation 10 for calculation of $\Delta\langle\rho_0^2\rangle$ another relation must be used:[17a,40]

$$\Delta\langle\rho_0^2\rangle = (\varphi_1\varphi_2 - \varphi_E/6)\Delta\langle\rho_{12}^2\rangle + (\varphi_2\varphi_3 - \varphi_E/6)\Delta\langle\rho_{23}^2\rangle + (\varphi_1\varphi_3 - \varphi_E/6)\Delta\langle\rho_{13}^2\rangle \quad (11)$$

Consequently, with the effect of the presence of transition layers on α accounted for, the value α' reflects the level of layered structure defect development. For the glassy-state polymer the value of α is 0.74 and increases to 0.9 after accounting for the presence of transition layers (Table I). Such a high value of α' (all more $\psi \sim 0.95$) indicates the presence in the polymer of one-dimensional translational order of a high degree of perfection which considerably exceeds the corresponding characteristics for smectic A and C mesophases.[26-28] Since during calculation we took into account the presence of a certain fraction of transition layers, the latter may be connected with a higher level of one-dimensional order in the arrangement of these layers and with less bending of the layer proper. The last statement is supported by comparison of electron-microscopic data for the polymer investigated and smectic A polymers.[45]

As is evident from the shape of $\rho(x)$ for the polymer investigated, it may be considered to be a three-component system with each component characterized by its level of electron density. This is a distinguishing feature of the smectic polymer with a long spacer group. Earlier for polymers with direct coupling of the mesogenic groups we have shown their two-component composition.[26]

According to data on electron density distribution $\rho(x)$ (Figure 8), the main chain polymer chains with side group fastening sections, the flexible spacers, and the rigid nuclei of the mesogenic groups appear as separate microphases within the total layered packing. Between these regions, depending of temperature, there exist transition layers ranging from 2 to 4 Å in thickness (Table I). It is probable that the isolation into separate microphases of macromolecular fragments of different nature is a necessary condition for the realization of a perfectly layered structure and is the cause of a principal difference between low and high molecular weight smectics, this difference being associated with the macromolecular nature and multicomponent composition of the latter. It confirms the concepts developed the last time in ref 26 and 40-42.

Nature of Correlation Damping and Layered-Pack Sizes. As is known, in a system with ideal periodicity the order in the arrangement of structural elements is established at macroscopic (as compared with separate element) distances. At the same time, as has been already noted above, the fluctuations of thermal motions of layers in one-dimensional systems with long-range order should lead to correlation damping in layer arrangement by the power law with value of $n = 0.1$–0.3 (see Introduction).[11,12] The presence of one-dimensional order with such a slow decrease of correlation in layer packing is a distinguishing feature of smectic phases in low molecular weight systems.[43,44]

A specific feature of the smectic polymer types A and C is the damping of correlations in layer arrangement by the exponential law with the value ξ (correlation length) being of the order of several tens of angstroms.[27,28] It means that in smectic polymers the one-dimensional order spreads only over 5–10 adjacent layers comprising a separate layered pack.[26-28,45] As can be seen from Figure 4, for a smectic of B type the correlation damping takes place considerably slower than in smectic polymers of A and C types. In the glassy state the correlation envelopes up to 23 adjacent layers, forming a layered pack of 680 Å in size. Consequently, in smectic A polymer the one-dimensional

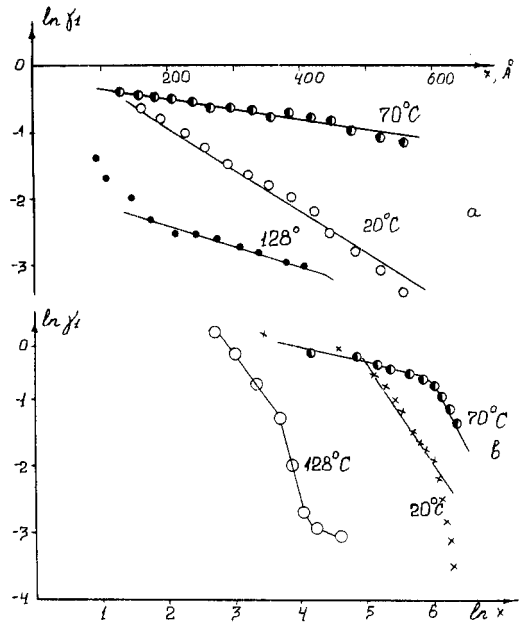

Figure 9. Nature of correlation damping in a polymer at various temperatures in semilogarithmic (a) and logarithmic (b) coordinates.

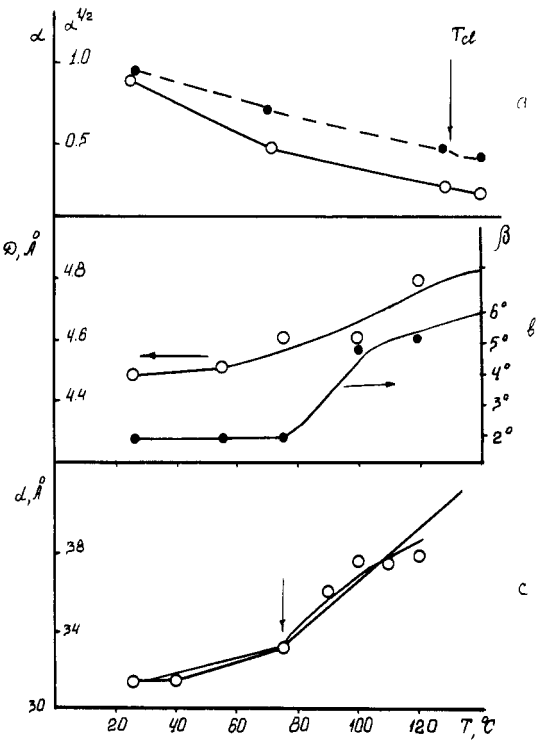

Figure 10. Temperature dependences of structural characteristic of a polymer: (a) segregation degree of components α (○) and ψ (●); (b) intralayer distance D and wide-angle maxima half-width β; (c) layer periodicity d (straight lines were used for estimation of K).

qausi-long-range order is practically realized in the packing of smectic layers. It is, probably, manifested also by the presence in this polymer of characteristic optical textures typical of smectic mesophases (Figure 1).[24] For smectic A and C polymers studied earlier by us only noncharacteristic small-grained texture could be obtained.

It is necessary to find out whether this leads to fundamental differences in the nature of correlation damping as compared with less-ordered smectics. Shown in Figure 9 is the dependence of the natural logarithm of the enveloping one-dimensional correlation functions on distance. In the case of an expontential damping, the dependence ln γ_1 on x should be presented by a straight line, whereas in the power law damping the dependence of ln γ_1 on ln x should be a linear nature. As can be seen from Figure 9, dependence ln $\gamma_1(x)$ for the polymer investigated is rectilinear, with the rectilinearity maintained throughout the entire range of mesophase existence. But in the ln γ_1–ln x plot may be seen a great curvature for all temperatures. Depending on temperature, the correlation length, determined from the slope of ln $\gamma_1(x)$ vs. x, varies within the limits of 160–600 Å (Table I), which is significantly higher than in corresponding smectic polymers of A and C types.

Thus, despite the presence of a perfectly layered structure in the smectic B polymer, it is characteristic of quite different laws governing the correlation damping in the layered structure than those in the low molecular weight smectics, these laws being characteristic of the other smectic polymers as well. The sharp damping of correlation in the packing of smectic layers may be connected with additional defects introduced by the polymeric main chains. But for clarification of this question additional experiments and theoretical works must be made.

Thermal Changes in Layered Order. As can be seen from Figure 2, with the rise of temperature to 70 °C considerable decrease of half-width of the SAXS maximum is observed (with a small decrease of its intensity), which may, naturally, be associated with the increase in the size of coherently scattering regions.[46] Actually, the corresponding correlation curves $G_1(x)$, in addition to the decrease in the height of maxima, exhibit a substantial decrease in their damping, so that $G_1(x)$ attains 0 only upon reaching the information zone of our diffractometer. Because of this, it becomes difficult to determine the true size of the layered pack for the polymer in LC state, and the low limit of 800 Å can be estimated. Close to T_{cl} (1 °C below it) the layered-pack size decreases considerably and, correspondingly, the correlation length decreases with it. Further on, during transition through T_{cl} the layered order becomes practically fully disturbed, so that the heights of maxima on $G_1(x)$ or $G_3(x)$ become very weak, their number drops to 2, the periodicity drops to 20 Å on $G_1(x)$ and 25 Å on $G_3(x)$, and the correlation length is only 15 Å. The correlation in the arrangement of structural elements is already damped at 40–50 Å.

The retention of weak maxima in the isotropic state is explained in a natural way within the limits of de Gennes' theory as the effect of "correlation hole" in systems consisting of bonded blocks of various electron densities.[47] In this case, even in the absence of ordering or segregation effects, a diffuse maximum will be observed on the scattering curve in the region of $s \sim 1/R$, where R is the size of a block differing from the other part of macromolecule by its electron density. In the case at hand, the fragments of the main chains, flexible spacers, and rigid nuclei appear as the elements of the block structure. The nonzero values of the electron density fluctuation in the isotropic state (without the thermal density fluctuation contribution) will, in these circumstances, be connected with the electron density variation from one block to another along the chain of macromolecules. Taking into account the fact that in the polymer studied these are, along the chains of side branches, two blocks of higher electron densities (rigid nuclei of mesogenic groups) totalling 22 Å in length, the appearance of a diffuse maximum in the isotropic phase at $R \approx 20$–25 Å is in full agreement with de Gennes' prediction.[47] But the absence of calculation of scattering-curve shapes for systems with rigid and flexible blocks does not

allow a final conclusion about the nature of this effect to be made.

The rise of temperature, as evident from Figure 10, results in the increase of the average intralayer distances D between the mesogenic groups by 10%, with the maximum increase being observed in the region of T_{cl}.[5] In parallel with this, the smectic layer thickness d increases by about 5%. Here the value of d rises, practically throughout the entire temperature interval (Figure 10). The increase of distances D and d with the rise of temperature is connected with thermal expansion of the layered and intralayer packings. The thermal expansion coefficient $K = [d(T) - d(T_0)]/[d(T_0)(T - T_0)]$ within the limits of the LC state is essentially lower for interlayer packing than that for the intralayer packing: 9×10^{-4} grad^{-1} and 4×10^{-4} grad^{-1}, respectively. This difference is much more than the accuracy in the determination of the K value (total error is less than 5%). The latter is attributed to the different nature of interaction between the neigboring atoms along and across the layer plane: along the normal-to-layer plane they are chemically bonded into one chain, whereas across the normal plane the van der Waals forces are acting.

As follows from Figure 8, characteristic thermal changes take place in the electron density distribution profile $\rho(x)$. The rise of temperature leads, first of all, to the reduction of the one-dimensional density wave amplitude and to the smoothing of packing densities in various microregions of a layered structure. The degree of segregation on α' drops in this case from 0.9 to 0.3 in the region of T_{cl}. In an isotropic melt α is retained at 0.18; maintenance of such high α in the isotropic melt indicates the above-mentioned features of heteropolymers connected with the correlation hole effect.

The retention of the initial shape of electron density $\rho(x)$ in a layered structure up to high temperatures is one of the interesting features of the systems under consideration. With the rise of temperatures, as can be observed in Figure 8, there is no essential $\rho(x)$ smearing along the normal-to-layer plane: the extent of higher density regions remains practically unchanged and the transition-zone thickness E does not exceed 4 Å (see Table I). This means that gradual distortion of the one-dimensional order due to temperature rise occurs mainly because of loosening of the intralayer packing of macromolecular fragments.

Conclusions

The above data on structural investigations of a smectic B polymer with long spacer groups make it possible to draw the following conclusions about the features of structural organization in polymer smectic of this type.

In the polymer studied, two-layered smectic structure is realized. The absence of diffraction, corresponding to this two-layered packing, is due to specific forms of electron density distribution, which leads to extinction of first-order reflection with d = 64 Å. As concluded, the detailed analysis of structural data for smectic polymers must be provided to avoid a discrepancy in interpretation of layered packing type.

In polymers with long spacer groups a microphase separation of different fragments takes place. As a result of microphase separation, three microregions in the layered structure with different densities appeared: they consist of main polymer chains with adjacent sections of side groups, rigid nuclei of side groups, rigid nuclei of mesogenic groups, and aliphatic spacer groups. Such electron density distribution permits one to refer to this polymer as a three-component system in which a separate packing of different macromolecular fragments occurs.

In smectic polymers with perfect intralayer packing (B type according to low molecular weight LC classification), the one-dimensional order in layer arrangement of a high degree of perfection is realized. The number of correlated layers in the polymer is 20–30, and the size of the layered packs reaches 600–800 Å.

Correlation damping in the arrangement of layers in the smectic B polymer obeys the exponential law. Correlation lengths for this polymer at various temperatures, as obtained, are several hundred angstroms, this being significantly higher than in ordered smectic of A and C types. An exponential law of correlation damping is a distinguishing feature of smectic as compared to their low molecular weight analogues.

The rise of temperature leads to an increase of layered and intralayer periodicity due to thermal expansion of the packing and to the decrease of one-dimentional density wave amplitude, as well as decreasing the perfection of smectic order due to distortion of intralayer packing. The thermal expansion of smectic structure is anisotropic: expansion along the normal-to-layer plane is less than expansion of intralayer packing. Preservation of diffuse maxima on the SAXS curve for a polymer in isotropic state may be connected with the presence in macromolecules of blocks with different electron density (so-called "correlation hole" effect).

Acknowledgment. We are grateful to Drs. Yu. Amerik and I. Konstantinov for samples of LC polymer. We are also indebted to O. Lokhonya for helpful assistance. We thank one of the referees for very helpful discussion concerning the extinction law for layered structures.

Registry No. $(H_2C{=}C(CH_3)CO_2(CH_2)_{10}CO_2\text{-}p\text{-}C_6H_4CO_2C_6H_4\text{-}p\text{-}OC_4H_9)_x$, 79704-56-6.

References and Notes

(1) Shibaev, V. P.; Plate, N. A. *Adv. Polym. Sci.* **1984**, *59*, 230.
(2) "Liquid Crystals of One- and Two-dimensional Order"; Helfrick, G. Heppke, Ed.; Springer-Verlag: Berlin, 1980.
(3) Shibaev, V. P.; Plate, N. A. *J. Chem. Soc. USSR* **1983**, *4*, 120.
(4) Lipatov, Yu. S.; Tsukruk, V. V.; Shilov, V. V.; Amerik, Yu. B.; Konstantinov, I. I. *Ukr. Phys. J.* **1982**, *27*, 209.
(5) Tsukruk, V. V.; Shilov, V. V.; Lipatov, Yu. S.; Grebneva, V. S.; Konstantinov, I. I.; Amerik, Yu. B. *Vysokomol. Soed., Ser. A* **1983**, *25*, 679.
(6) Lipatov, Yu. S.; Tsukruk, V. V.; Shilov, V. V.; Amerik, Yu. B.; Konstantinov, I. I. In "Advances in Liquid Crystal Research and Applications"; Bata, L., Ed.; Pergamon Press: New York, 1980; Vol. 2, p 943.
(7) Tsukruk, V. V.; Shilov, V. V.; Grebneva, V. S.; Konstantinov, I. I.; Amerik, Yu. B. *Mol. Cryst. Liq. Cryst.* **1982**, *82*, 215.
(8) de Gennes, P.-G. "Physics of Liquid Crystals"; Claredon Press: London, 1975.
(9) Giylon, D.; Poetry, G.; Skulious, A.; Fanelli, E., *J. Phys., Lett.*, **1983**, *44*, 491.
(10) Gunter, L.; Imry, J.; Lajerovitsz, J. *Phys. Rev. A* **1980**, *A22*, 1733.
(11) Landau, L. D. "Selected Works"; Nauka: Moscow, USSR, 1965; Vol. I.
(12) Galle, A. *C. R. Seances Acad. Sci., Ser B* **1972**, *B274*, 891.
(13) Debye, P.; Bueche, A. M. *J. Appl. Phys.* **1949**, *20*, 518.
(14) Vonk, K. J. *J. Appl. Crystallogr.* **1978**, *11*, 541.
(15) Amerik, Yu. B.; Krentsel, B. A. "Chemistry of Liquid Crystals and Mesomorphic Polymers"; Nauka: Moscow, 1981.
(16) Konstantinov, I. I.; Grebneva, V. S.; Sitnov, A. V. In "Abstracts, First All-Union Symposium on LC Polymers", Suzdal, 1982; Nauka: Moscow, 1982; p 16 (in Russian).
(17) (a) Lipatov, Yu. S.; Shilov, V. V.; Gomza, Yu. P.; Kruglyak, N. E. "X-ray Methods of Polymer System Investigations"; Naukova Dumka: Kiev, 1982, (in Russian). (b) "Small-angle X-ray Scattering"; Glatter, O.; Kratky, O., Ed.; Academic Press: New York, 1982. (c) Roe, R. J. *J. Appl. Crystallogr.* **1982**, *15*, 182. (d) Hasimoto, T.; Fujimura, M.; Kawai, H. *Macromolecules* **1980**, *13*, 1660. (e) Shilov, V. V.; Tsukruk, V. V.; Lipatov, Yu. S. *Vysokomol. Soedin., Ser. A* **1984**, *26*, 1347.
(18) Kratky, O.; Pilz, I. *Q. Rev. Biophys.* **1972**, *5*, 481.
(19) Schmidt, P. V. *Acta Crystallogr.* **1971**, *19*, 938.

(20) Crist, B. *J. Polym. Sci., Polym. Sci., Polym. Phys. Ed.* **1973**, *11*, 635.
(21) Hosemann, R.; Bredin, O. W. *Chem. Techn. Cell.* **1980**, *14*, 583.
(22) Vonk, C. J.; Kortleve, G. *Kolloid Z. Z. Polym.* **1967**, *220*, 19.
(23) Vonk, C. *J. Appl. Crystallogr.* **1975**, *8*, 340.
(24) Demus, D.; Richter, L. "LC Textures"; VEB Fachbuchverlag: Leipzig, 1980.
(25) Shilov, V. V.; Tsukruk, V. V.; Bliznyuk, V. N.; Lipatov, Yu. S. *Polymer* **1982**, *23*, 484.
(26) Lipatov, Yu. S.; Tsukruk, V. V.; Shilov, V. V. *Polym. Commun.* **1983**, *24*, 75.
(27) Tsukruk, V. V.; Shilov, V. V.; Lipatov, Yu. S. *Eur. Polym. J.* **1983**, *19*, 199.
(28) Lipatov, Yu. S.; Shilov, V. V.; Tsukruk, V. V. *Ukr. Phys. J.* **1983**, *28*, 543.
(29) Plate, N. A.; Shibaev, V. P. "Comb-like Polymers and Liquid Crystals"; Nauka: Moscow, 1980 (in Russian).
(30) Blumstein, A.; Klug, S.; de Vries, A. *Polym. Prepr. (Am. Chem. Soc.-Div. Polym. Chem.* **1977**, *17*, 1.
(31) Tsukruk, V. V.; Shilov, V. V.; Lipatov, Yu. S.; Konstantinov, I. I.; Amerik, Yu. B. *Acta Polym.* **1982**, *33*, 63.
(32) Strobl, G. R.; Schneider, M. *J. Polym. Sci., Polym. Phys. Ed.* **1980**, *18*, 1343.
(33) Hosemann, R.; Bagchi, S. "Direct Analysis Diffraction by Matter"; North-Holland: Amsterdam, 1962.
(34) Tsukruk, V. V.; Shilov, V. V.; Lipatov, Yu. S. *Crystallogr.*, in press.
(35) Vonk, C. J. *J. Appl. Crystallogr.* **1973**, *6*, 81.
(36) Hashimoto, T.; Shibayama, M.; Kawai, N. *Macromolecules* **1980**, *13*, 1237.
(37) Roe, R. J.; Fishkis, M.; Chang, J. S. *Macromolecules* **1981**, *14*, 1091.
(38) Lipatov, Yu. S. "Interphase Phenomena in Polymers"; Naukova Dumka: Kiev, USSR, 1980 (in Russian).
(39) Bonart, R.; Muller, E. H. *J. Macromol. Sci. Phys.* **1974**, *10*, 345.
(40) Koberstein, L. Stein, R. *J. Polym. Sci., Polym. Phys. Ed.* **1983**, *21*, 1439.
(41) Tsukruk, V. V.; Shilov, V. V.; Lipatov, Yu. S. *Makromol. Chem.* **1982**, *183*, 2009.
(42) Cser, F. In "Abstracts, Fourth Conference on Liquid Crystals", Tbilisi, 1981; Nauka: Moscow, 1981; Vol. 2, p 190.
(43) Davidov, D.; Safiniy, C. R.; Kaplan, M.; Dana, S. S.; Litster, J. D. *Phys. Rev.* **1979**, *B19*, 1657.
(44) Safiniy, C. R.; Kaplan, M.; Als-Neisen, J.; Birgenau, R. J.; Davidov, D.; Litster, Y. D. *Phys. Rev. B: Condens. Matter* **1980**, *B21*, 4149.
(45) Lipatov, Yu. S.; Tsukruk, V. V.; Shilov, V. V. *J. Macromol. Sci., Rev. Macromol. Chem. Phys.* **1984**, *24*, 173.
(46) Vainstein, B. K. "X-ray Diffraction on Chain Molecules"; Nauka: Moscow, 1963 (in Russian).
(47) de Gennes, P. "Concepts in Scaling in Polymer Physics"; Cornell University Press: Ithaca, NY, 1979.
(48) Tsukruk, V.; Shilov, V.; Lipatov, Yu. *J. Polym. Sci., Polym. Phys. Ed.* **1984**, *22*, 41.

From Plastic-Crystal Paraffins to Liquid-Crystal Polyethylene: Continuity of the Mesophase in Hydrocarbons

Goran Ungar

H. H. Wills Physics Laboratory, Bristol BS8 1TL, England, and Rudjer Boškovič Institute, POB 1016, Zagreb, Yugoslavia. *Received December 4, 1985*

ABSTRACT: The relationship is explored between the plastic "rotator" phase (RP), which occurs in *n*-alkanes up to C_{40}, and the "liquid-crystalline" high-pressure hexagonal phase (HPHP) in polyethylene. The radiation-induced hexagonal phase (RIHP) of polyethylene, which is intermediate between the two, has been shown in a previous study to behave with increasing pressure essentially like HPHP. In this work a link is demonstrated between RP and RIHP through a study of paraffin C_{11}, binary paraffins C_{23}–C_{25} and C_{36}–C_{40}, as well as irradiated polyethylene by Fourier-transform infrared spectroscopy. Absence of GG defects and presence of GTG* kinks was confirmed in both RP and RIHP. A smooth continuity was established between the two phases by the defect concentration criterion. More evidence for such continuity is provided by a systematic comparison of published pressure–temperature diagrams for paraffins and polyethylenes. Moreover, the available data for high-temperature forms in related systems (high-modulus polyethylene fibers, cycloalkanes, and substituted *n*-alkanes) all suggest that a single master relation between the degree of order and variables such as temperature and chain stem length can, to a good approximation, describe the qualitative behavior of the wide range of hexagonal or pseudohexagonal phases in hydrocarbon chain systems.

Introduction

n-Alkanes up to tetracontane (C_{40}) undergo on heating a strong first-order transition a few degrees below the melting point into the so-called rotator phase (RP). This has been extensively studied both experimentally[1–12] and theoretically[13–16] partly because of the importance of RP in understanding the order and mobility in chain molecular systems and partly because of its direct relevance to phase behavior in phospholipid layers[17] and, recently, in Langmuir–Blodgett films.[18]

Quite independently of the research on paraffins, studies were performed on the high-pressure hexagonal phase (HPHP) in polyethylene.[19–26] The two phenomena have mostly been treated separately and have generally been considered to be qualitatively different.

The distinction between RP and HPHP originates from the following. The earlier studies of RP were mainly performed on relatively short paraffins, around 20 C atoms long. X-ray diffraction[1] and Raman spectroscopy[2] indicated that chains retain their all-trans conformation in RP, the disorder being accounted for by hindered rotation around the chain axis together with a degree of translational motion.[12] The nearest description of RP would thus be that of a plastic-crystal state. In contrast, HPHP is considered to contain a large proportion of gauche bonds. Largely on the basis of the similarity of Raman spectra of HPHP and the melt,[23] it was concluded that the chain conformation in HPHP does not differ significantly from that in the melt. Further, while the ratio of entropies of the orthorhombic–hexagonal (o–h) and hexagonal–melt (h–m) transitions in paraffins ranges from $(s_h - s_o)/(s_m - s_h) = 0.3–0.6$,[27] in polyethylene at high pressures this ratio is around 3.[22] HPHP has accordingly been described as a liquid crystal[28] or a "condis" (conformationally disordered) crystal form.[29]

The different behavior of RP and HPHP with increasing pressure has been taken as a further distinguishing feature: while RP disappears with increasing pressure, HPHP is

0024-9297/86/2219-1317$01.50/0